Pergamon

Geochimica et Cosmochimica Acta, Vol. 67, No. 15, pp. 2763–2774, 2003

0016-7037/03 $30.00 + .00

doi:10.1016/S0016-7037(00)00091-7

# Aqueous cadmium uptake by calcite: A stirred flow-through reactor study

A. MARTIN-GARIN,[1,†] P. VAN CAPPELLEN,[2,*] and L. CHARLET[3]

[1]Section des Applications des Traceurs, Atomic Energy Commission, CEA, 38054 Grenoble Cedex 9, France
[2]Department of Geochemistry, Faculty of Earth Sciences, Utrecht University, P.O. Box 80021, 3508 TA Utrecht, The Netherlands
[3]Environmental Geochemistry Group, LGIT-IRIGM, University of Grenoble I, B. P. 53, 38041 Grenoble Cedex 9, France

(*Received April* 15, 2002; *accepted in revised form January* 23, 2002)

**Abstract**—Uptake of cadmium ions from solution by a natural Mg-containing calcite was investigated in stirred flow-through reactor experiments. Input NaCl solutions were pre-equilibrated with calcite (pH 8.0) or not (pH 6.0), prior to being spiked with $CdCl_2$. For water residence times in the reactor less than 0.5 h, irreversible uptake of Cd by diffusion into the bulk crystal had a minor effect on the measured cadmium breakthrough curves, hence allowing us to quantify "fast" $Cd^{2+}$ adsorption. At equal aqueous activities of $Cd^{2+}$, adsorption was systematically lower for the pre-equilibrated input solutions. The effect of variable solution composition on $Cd^{2+}$ adsorption was reproduced by a $Ca^{2+}$-$Cd^{2+}$ cation exchange model and by a surface complexation model for the calcite-aqueous solution interface. For the range of experimental conditions tested, the latter model predicted binding of aqueous $Ca^{2+}$ and $Cd^{2+}$ to the same population of carbonate surface sites. Under these circumstances, both adsorption models were equivalent. Desorption released 80 to 100% of sorbed cadmium, confirming that fast uptake of $Cd^{2+}$ was mainly due to binding at surface sites. Slow, irreversible cadmium uptake by the solid phase was measured in flow-through reactor experiments with water residence times exceeding 0.7 h. The process exhibited first-order kinetics with respect to the concentration of adsorbed $Cd^{2+}$, with a linear rate constant at 25°C of 0.03 $h^{-1}$. Assuming that diffusion into the calcite lattice was the mechanism of slow uptake, a $Cd^{2+}$ solid-state diffusion coefficient of $8.5\times10^{-21}$ $cm^2$ $s^{-1}$ was calculated. Adsorbed $Cd^{2+}$ had a pronounced effect on the dissolution kinetics of calcite. At maximum $Cd^{2+}$ surface coverage ($\sim10^{-5}$ mol $m^{-2}$), the calcite dissolution rate was 75% slower than measured under initially cadmium-free conditions. Upon desorption of cadmium, the dissolution rate increased again but remained below its initial value. Thus, the calcite surface structure and reactivity retained a memory of the adsorbed $Cd^{2+}$ cations after their removal. 

## 1. INTRODUCTION

Because of their importance in controlling the fate and mobility of contaminants and nutrients in the environment, processes at the mineral–water interface have been studied extensively. Carbonate minerals are of particular interest because they are widespread in soils, shallow aquifers and sediments. The interactions of dissolved cadmium ions with calcite surfaces have been the subject of many studies in the last 20 yr (McBride, 1980; Lorens, 1981; Davis et al., 1987; Papadopoulos and Rowell, 1988; Königsberger et al., 1991; Zachara et al., 1991; Stipp et al., 1992; van der Weijden, 1995; Reeder, 1996; Tesoriero and Pankow, 1996; Chiarello et al., 1997). Both macroscopic studies and, more recently, studies involving high-resolution methods for in situ surface analysis, have demonstrated the high affinity of $Cd^{2+}$ ions for calcite.

Cadmium uptake from aqueous solution by calcite usually consists of two steps: rapid chemisorption followed by slower uptake. Recent studies have mainly focused on the second step, which is generally thought to correspond to the formation of an otavite–calcite solid solution, probably by a combination of co-precipitation and solid-state diffusion of surface ions into the bulk lattice. Researchers have aimed at determining the composition, thermodynamics and kinetics of the $CdCO_3$-$CaCO_3$ surface precipitates to assess their significance for Cd immobilization in natural environments. The recent trend in experimental studies shows that macroscopic (solution-based) measurements combined with surface spectroscopic plus microscopic experiments offer a powerful approach to unravel mineral-solute interactions (Stipp et al., 1992; Scheidegger and Sparks, 1996; Chiarello et al., 1997; Sturchio et al., 1997).

The objective of the present work was to contribute to the establishment of a consistent thermodynamic and kinetic data base for solution-mineral interactions in the calcite-$H_2O$-Cd(II) system. To this end we used stirred flow-through reactors which allowed us to separate adsorption of $Cd^{2+}$ at the surface of calcite from uptake due to incorporation in the existing crystal lattice or formation of a new (surface) phase. Thus, both $Cd^{2+}$ adsorption isotherms and rates of "slow" $Cd^{2+}$ uptake were measured experimentally. In addition, the effects of $Cd^{2+}$ adsorption on the dissolution kinetics of calcite were determined.

## 2. BACKGROUND

### 2.1. Sorption

Removal of a chemical species from solution in the presence of particulate matter may reflect a variety of molecular processes, including adsorption, absorption, precipitation and co-precipitation. Following Sposito (1986), adsorption sensu stricto is defined as the "accumulation of matter at the interface between the aqueous solution phase and a solid adsorbent without the development of a three-dimensional molecular arrangement." The other uptake mechanisms imply a three-di-

* Author to whom correspondence should be addressed (pvc@geo.uu.nl).
†*Present address:* Laboratory of Experimental Radioecology, Institute of Radioprotection and Nuclear Safety, CE Cadarache, B.P.1, 13108 Saint Paul Lez Durance Cedex, France.

mensional redistribution of the sorbate species in the existing sorbent (absorption), or the formation of a new solid phase (surface precipitation, co-precipitation).

The initial "fast" uptake of an aqueous metal cation by a mineral surface is generally ascribed to reversible adsorption at the interface and, hence, is represented by thermodynamic equilibrium distribution models. The characteristic time scale of metal adsorption on mineral surfaces is typically on the order of minutes (McBride, 1980; Davis et al., 1987; Papadopoulos and Rowell, 1988). Frequently, adsorption is followed by a slow removal of dissolved cations on time scales of hours to days. This slow removal may be due to surface precipitation, co-precipitation, or diffusion of the previously adsorbed cations into the existing solid (for a review, see Charlet, 1994). Either co-precipitation or solid-state diffusion may result in the formation of a solid-solution (Stipp et al., 1992). An important factor controlling the reversibility of metal uptake and the relative importance of slow versus fast uptake is the contact time between solid and metal.

### 2.2. Cadmium–Calcite Interactions

Aqueous cadmium ions have a strong affinity for calcite. For divalent metal cations, Zachara et al. (1991) proposed the following order of uptake affinity on calcite: $Cd > Zn \geq Mn > Co > Ni \gg Ba \approx Sr$. They accounted for the sequence based on the ionic radii of the $Me^{2+}$ cations and the solubility products of the $MeCO_3$ solids. Ion exchange of $Cd^{2+}$ for $Ca^{2+}$ at the mineral–water interface (McBride, 1980; Davis et al., 1987), defect-enhanced diffusion into the lattice (Stipp et al., 1992), and co-precipitation (McBride, 1980; Davis et al., 1987; Zachara et al., 1991) have all been proposed as possible uptake mechanisms of aqueous cadmium by calcite. The formation of $CaCO_3$-$CdCO_3$ solid-solutions and the epitaxial growth of otavite on calcite, as a result of cadmium uptake from solution, have been confirmed by spectroscopic techniques (Stipp et al., 1992; Chiarello and Sturchio, 1994). Chang and Brice (1971), Königsberger et al. (1991) and Tesoriero and Pankow (1996) further showed that otavite and calcite are completely miscible at room temperature.

At equilibrium, partitioning of $Cd^{2+}$ between the aqueous phase and the otavite–calcite solid-solution is described by the partitioning coefficient, $D$,

$$D = \frac{X_{CdCO_3}[Ca^{2+}]}{X_{CaCO_3}[Cd^{2+}]} \quad (1)$$

where $[Ca^{2+}]$ and $[Cd^{2+}]$ represent aqueous ion concentrations, and $X_{CdCO3}$ and $X_{CaCO3}$ the mole fractions of $CdCO_3$ and $CaCO_3$ in the solid solution. For an ideal solid solution, the partition coefficient equals the ratio of the solubility constants, $K_{so}$, of the pure end-members, calcite and otavite, assuming that aqueous $Cd^{2+}$ and $Ca^{2+}$ have identical activity coefficients. At 25°C, the predicted value of Log $D$ varies between 2.8 and 3.6, depending on the choice of $K_{so}$ for cadmium carbonate (Davis et al., 1987; Tesoriero and Pankow, 1996). Measured values of Log $D$ lie in the range 3.0 to 3.7 (Lorens, 1981; Davis et al., 1987; Papadopoulos and Rowell, 1988; Tesoriero and Pankow, 1996).

The studies of Davis et al. (1987) and Stipp et al. (1992) have highlighted the continuum between fast adsorption of dissolved $Cd^{2+}$ onto calcite surfaces and its subsequent non-reversible solid-phase incorporation. Batch reactor experiments by Davis et al. (1987) showed no dependence of the rate of the slow incorporation process on the amount of adsorbed $Cd^{2+}$. These authors observed constant removal rates of dissolved $Cd^{2+}$ for durations of up to 150 h. The fraction of sorbed cadmium that could be desorbed was found to decrease with increasing contact time between the calcite crystals and solution suggesting incorporation in the bulk solid. Using XPS and LEED, Stipp et al. (1992) showed that surface precipitation and diffusion into the lattice lead to non-reversible sequestration of cadmium by calcite.

### 2.3. Equilibrium Adsorption Modeling

According to McBride (1980), Davis et al. (1987), Papadopoulos and Rowell (1988), and Zachara et al. (1991), cadmium chemisorption onto calcite surfaces can be described by an equilibrium surface-exchange reaction between calcium and cadmium cations,

$$Ca_{solid} + Cd^{2+} \Leftrightarrow Cd_{solid} + Ca^{2+} \quad (2)$$

where $Me_{solid}$ refers to surface lattice calcium and cadmium ions. The exchange constant of the reaction, $K_{ex}$, is defined as,

$$K_{ex} = \frac{(Ca^{2+})}{(Cd^{2+})}\left[\frac{X_{Cd}}{X_{Ca}}\right]^n \quad (3)$$

where $n$ is an empirical coefficient, and $(Me^{2+})$ and $X_{Me}$ (Me = Ca, Cd) correspond to the aqueous activity and mole fraction of cation surface lattice sites occupied by $Me^{2+}$, respectively. When n = 1, the exchange reaction may be considered ideal (Zachara et al., 1991) and $K_{ex}$ is equivalent to the conditional equilibrium constant $c_{K_{ex}}$. Reported values of Log $c_{K_{ex}}$ range between 3.02 to 3.20 (Davis et al., 1987; Zachara et al., 1991; van der Weijden, 1995). If an ideal solid solution forms in equilibrium with the aqueous phase, $c_{K_{ex}}$ equals $D$.

Van Cappellen et al. (1993) developed an alternative model for cation adsorption at the carbonate mineral-aqueous solution interface. This surface complexation model postulates the existence of hydration species $>CO_3H^0$ and $>MeOH^0$ at the surface of a divalent metal carbonate, $MeCO_3$ (the symbol $>$ represents the surface lattice). Spectroscopic evidence for the formation of these surface species has been presented for calcite and dolomite (Stipp and Hochella, 1991; Pokrovsky et al., 1998; Fenter et al., 2000). In the surface complexation approach, reactions between the surface hydration species and dissolved species account for the chemical structure and reactivity of the carbonate mineral-solution interface. The surface reactions are written in analogy with acid-base and complexation reactions in homogeneous solution (Table 1). The model has been applied successfully to explain the development of surface charge and the dissolution kinetics of a number of carbonate minerals in terms of the densities of surface species (Van Cappellen et al., 1993; Arakaki and Mucci, 1995; Nilsson and Sternbeck, 1999; Pokrovsky and Schott, 1999; Pokrovsky et al., 1999).

Here, we apply the constant capacitance surface complexation model of Van Cappellen et al. (1993), using the intrinsic surface stability constants and electric double layer capacitance

Table 1. Surface complexation reactions and corresponding intrinsic stability constants in the system $CaCO_3$(calcite)-$H_2O$-$CO_2$ (from Van Cappellen et al., 1993). $\kappa$ represents the constant capacitance of the electric double layer (EDL).

| Surface reactions | | Log K 25°C, 1 atm, I = 0 |
|---|---|---|
| $>CaOH^O + H^+ \Leftrightarrow >CaOH_2^+$ | (4) | 12.2 |
| $>CaOH^o \Leftrightarrow >CaO^- + H^+$ | (5) | −17 |
| $>CaOH^o + CO_3^{2-} + 2H^+ \Leftrightarrow >CaHCO_3^o + H_2O$ | (6) | 24.15 |
| $>CaOH^o + CO_3^{2-} + H^+ \Leftrightarrow >CaCO_3^- + H_2O$ | (7) | 15.55 |
| $>CO_3H^o \Leftrightarrow >CO_3^- + H^+$ | (8) | −4.9 |
| $>CO_3H^o + Ca^{2+} \Leftrightarrow >CO_3Ca^+ + H^+$ | (9) | −2.8 |

$\kappa$ = 17 F $m^{-2}$, from $\kappa = (\sqrt{I}/\alpha)$, with $\alpha$ = 0.006 and I (ionic strength) = $10^{-2}$ mol $dm^{-3}$

given in Table 1, and the aqueous stability constants listed in the Appendix. The following two reactions were used to describe cadmium adsorption onto calcite surfaces:

$$>CO_3H^0 + Cd^{2+} \Leftrightarrow >CO_3Cd^+ + H^+ \quad (10)$$

$$>CaOH^0 + Cd^{2+} \Leftrightarrow >CaOCd^+ + H^+ \quad (11)$$

It should be noted that other types of adsorption complexes have been postulated, with different bonding configurations or involving adsorbed Cd complexes, such as $CdCl^+$ or $CdOH^+$. For the sake of simplicity, only the representations of surface complexes given by Eqns. 10 and 11 are considered here.

### 2.4. Stirred Flow-Through Reactor

Flow-through reactors (Fig. 1) are particularly useful for studying mineral–water reaction kinetics (e.g., Nagy and Lasaga, 1992; Van Cappellen and Qiu, 1997a,b). By varying the composition of the inlet solution and the flow rate, steady-state rates can be measured over a wide range of solution composition. In addition, breakthrough experiments can be performed to measure the adsorption and desorption of chemical species in the presence of a suspended solid (e.g., Grolimund et al., 1995).

In a perfectly stirred flow-through reactor, the solution composition is homogeneous within the reactor and equal to that measured in the outlet flow. For an inert (i.e., non-reactive) solute species, the breakthrough curve (BTC), that is, the evolution with time of the outlet concentration, $C$, after a step-wise increase of the input concentration from 0 to $C_0$, is given by (Villermaux, 1985):

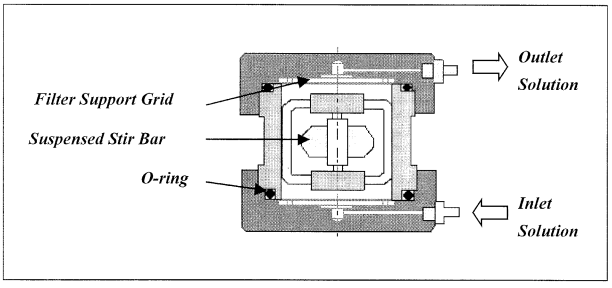


Fig. 1. Stirred flow-through reactor.

$$C(t) = C_0\left[1 - \exp\left(-\frac{Q}{V_r}t\right)\right] \quad (12)$$

where $Q$ represents the flow rate, $V_r$, the reactor volume, and $t$, time. The ratio $V_r/Q$ defines the water residence time in the reactor. For a reactive species, the BTC deviates from that predicted by Eqn. 12. In the case of aqueous $Cd^{2+}$ uptake by calcite particles suspended in the reactor, the amount of sorbed cadmium is given by the surface area separating the observed $Cd^{2+}$ BTC and the tracer BTC (Eqn. 12). In this study, the measured outflow concentrations of $Cd^{2+}$ were fitted to a cubic splines function, which was then integrated with time to obtain the surface area under the BTC.

After steady state is reached in a flow-through experiment, the total dissolved cadmium concentration, $[Cd]_{ss}$, in the outlet flow remains constant. For experimental conditions where the water residence time in the reactor is much shorter than the characteristic time scale of "slow" $Cd^{2+}$ uptake, $[Cd]_{ss}$ is equal to the input concentration, $[Cd]_0$. Such conditions can always be created by increasing the flow rate, $Q$, to a sufficiently high level. The difference in the BTC of dissolved $Cd^{2+}$ and that of an inert tracer then only reflects $Cd^{2+}$ removal by "fast" adsorption to calcite. From the amount of $Cd^{2+}$ removed from solution, the surface density of adsorbed $Cd^{2+}$ in equilibrium with the dissolved concentration $[Cd]_0$ can be calculated (Grolimund et al., 1995). Reversibility can be tested by switching back to a cadmium-free input solution, hence, forcing adsorbed $Cd^{2+}$ to desorb.

By adjusting $Q$ to a sufficiently slow value, a steady state can be reached for which $[Cd]_{ss} < [Cd]_0$. The persistent concentration difference between inflow and outflow then indicates a continued removal of $Cd^{2+}$ by "slow," non-equilibrium uptake. The rate of "slow" uptake is given by

$$R_{Cd} = \frac{Q([Cd]_0 - [Cd]_{ss})}{SA\ m_{calcite}} \quad (13)$$

where $SA$ and $m_{calcite}$ denote the specific surface area and mass of calcite, and $R_{Cd}$ is expressed in mol $m^{-2}$ $h^{-1}$.

## 3. MATERIALS AND METHODS

### 3.1. Calcite

Experiments were conducted with a natural calcium carbonate, Mikhart130 from Provençale S.A. (Cases de Pene, France). The X-ray diffraction pattern was indistinguishable from that of pure calcite. The raw product was sieved and the size fraction between 100 and 140 $\mu$m was rinsed repeatedly with ultra-pure water to remove fine particles. The effectiveness of the washing procedure was verified by scanning electron microscopy (Fig. 2). The specific surface area of the washed product was 0.20 $m^2$ $g^{-1}$, as determined by the $N_2$-BET technique (precision ±10%). Mechanical stirring during the experiments caused a slight change in surface area of the calcite grains. In blank tests, the specific surface area was found to increase to 0.28 $m^2$ $g^{-1}$ after 48 h of continuous stirring. The latter value was used in the calculations.

Chemical analysis, performed by ICP-MS, indicated the presence of $Mg^{2+}$ (1.2%) and, to a lesser extent, $Fe^{2+}$ (0.03%) in the calcite. Cadmium concentrations in the solid were below detection. The calcite solubility product was calculated from the composition of equilibrated solutions, following the approach of Thorstenson and Plummer (1977). The experimental value, Log $K_{so}$ = 9.3 ± 0.1, was higher than that of pure calcite, as expected for a Mg-containing calcite (Busenberg and Plummer, 1989; Mucci, 1986).

The calcite was stored in a 0.01 mol/L NaCl solution, to avoid artefacts due to exposure to air (Stipp et al., 1996). All experiments reported in this study were performed with the same calcite stock suspen-

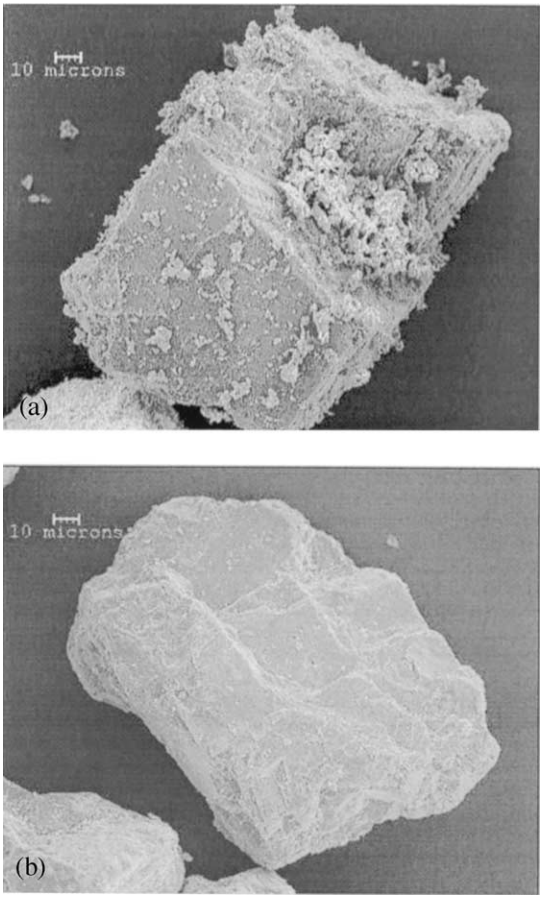


Fig. 2. Scanning electron micrographs of calcite grains before (a) and after (b) repeated washing with ultra-pure water.

sion. The solid concentration of the suspension (50 g $dm^{-3}$) was determined by weighing four replicate samples after evaporation. Addition of calcite to the reactors was done by measuring out a precise volume of the homogenized stock suspension. Experiments were run with 0.12 ± 0.01 g initial mass of calcite in the reactors. The total amount of calcite dissolved during the flow-through experiments never exceeded 5% of the initial mass. Hence, as a first approximation, the mass of calcite in the reactor during experiments was assumed to remain constant.

### 3.2. Solutions

Input solutions were prepared with Ultrapure water (18 MΩ resistivity) and reagent-grade chemicals. They were either preequilibrated with the calcite, or not: the two types of solution are identified as EqW and NEqW, respectively. EqW solution was prepared by reacting Ultrapure water with the natural calcite, in contact with atmospheric $CO_2$. Periodic sampling confirmed that the solution reached equilibrium within 1 month. A large quantity of EqW solution was synthesized. Before each experiment, the required amount of solution was filtered through 0.45 μm pore size membranes and analyzed for calcium concentration, pH and alkalinity. The ionic strength of EqW and NEqW solutions was adjusted to 0.01 mol $dm^{-3}$ by NaCl. Table 2 gives the compositions of the input solutions.

The solutions were spiked with cadmium (as $CdCl_2$) to obtain input solutions with total cadmium concentrations between $2.2\times10^{-9}$ and $4.5\times10^{-4}$ mol $dm^{-3}$. A number of experiments were carried out using $^{109}$Cd radioactive tracer (γ-emission, 88 keV, $T_{1/2}$ = 462 d). A small quantity of $^{109}$Cd was added to EqW and NEqW solutions to create specific activities of $\sim4.0\times10^{5}$ Bq $dm^{-3}$. The acidity of the spiking solution was neutralized by 0.1 mol $dm^{-3}$ NaOH.

Table 2. Compositions of inflow solutions.[a]

| | NEqW | EqW |
|---|---|---|
| $Ca^{2+}$ | 0 | $2.6 \pm 0.2 \times 10^{-4}$ |
| Alkalinity | $2.4 \times 10^{-5}$ | $5.0 \pm 0.5 \times 10^{-4}$ |
| pH | 5.7 | 8.0 ± 0.1 |
| Ionic strength[b] | $10^{-2}$ | $10^{-2}$ |

[a] EqW = solution equilibrated with calcite at 25°C and atmospheric $CO_2$; NEqW = solution not equilibrated with calcite; concentrations in mol $dm^{-3}$.
[b] Ionic strength adjusted with NaCl.

### 3.3. Flow-Through Experiments

The flow-through reactors (Fig. 1, modified after Van Cappellen, 1997), had an internal volume ($V_r$) of 36 $cm^3$. Aqueous solution entered and left the reactors through 0.45 μm pore size hydrofoil Teflon membranes (HVLP, Millipore). Blank tests with highly sensitive $^{109}$Cd analyses did not reveal any significant $Cd^{2+}$ sorption by the reactor materials or filters. Flow through the reactors was controlled by mechanical piston pumps (Pharmacia P-500). A range of flow rates between 10.0 ± 0.1 and 100 ± 2 $cm^3$ $h^{-1}$ was used, with corresponding solution renewal rates between 0.3 and 2.8 $V_r$ $h^{-1}$. Flow rates were stable throughout the experiments. The calcite-solution suspension in the reactor was continuously stirred by a magnetic Teflon bar. The outflow solutions were monitored on-line for pH and conductivity. Samples were collected with a fraction collector and analyzed for cadmium, calcium and alkalinity.

Dissolved calcium concentrations were measured by AAS. Alkalinity was measured by titration with $10^{-3}$ mol $dm^{-3}$ HCl, following the Gran method (Stumm and Morgan, 1981). Dissolved cadmium concentrations were determined by ICP-MS or by gamma scintillation-counting for $^{109}$Cd-spiked experiments. In the latter case, the dissolved cadmium concentration was derived from the relative difference in activity between input and output solutions. Counting times were adjusted to achieve accuracies >99%.

In the flow-through experiments with NEqW input solutions, undersaturated conditions caused calcite to dissolve. Because the input solution contained no dissolved calcium (Table 2), the calcium concentration in the outflow, $[Ca]_{out}$, provided a direct measure of the rate of calcite dissolution:

$$R = \frac{Q[Ca]_{out}}{m_{calcite}} \quad (14)$$

where the rate, R, is given in mol $g^{-1}$ $h^{-1}$.

The experiments were carried out at 25.0 ± 0.5 C°, with reactors immersed in a water bath. Before each experiment, the reactor was washed with 5% nitric acid solution, then rinsed with Ultrapure water. The performance of the reactors was tested by imposing a step-change from Ultrapure water to a $10^{-2}$ mol $dm^{-3}$ NaCl solution and measuring the conductivity BTC in the output solution. The conductivity tracer experiments were performed in the presence and absence of calcite.

Cadmium uptake experiments on calcite were performed with NEqW and EqW solutions in the following sequence. (Stage I) A Cd-free solution was pumped through the reactor until steady state was reached. (Stage II) The input was switched to a Cd-containing solution with an otherwise identical composition to that of the initial solution. The Cd-containing solution was supplied at a constant flow rate until steady state was reached. (Stage III) In a number of experiments, cadmium desorption was monitored by switching back to the initial Cd-free solution. Figure 3 shows the results of a typical sorption-desorption experiment. Also given in the figure are the variations of calcium concentration, total alkalinity, conductivity and pH of the outlet solution. Tables 3 and 4 summarize the experimental conditions and results of all the flow-through experiments. Blank Cd breakthrough experiments were performed with reactors containing no calcite.

## 4. RESULTS

### 4.1. Reactor Hydrodynamics

An experimental inert tracer breakthrough curve (BTC) is compared to the theoretical BTC (Eqn. 12) in Figure 4. Note

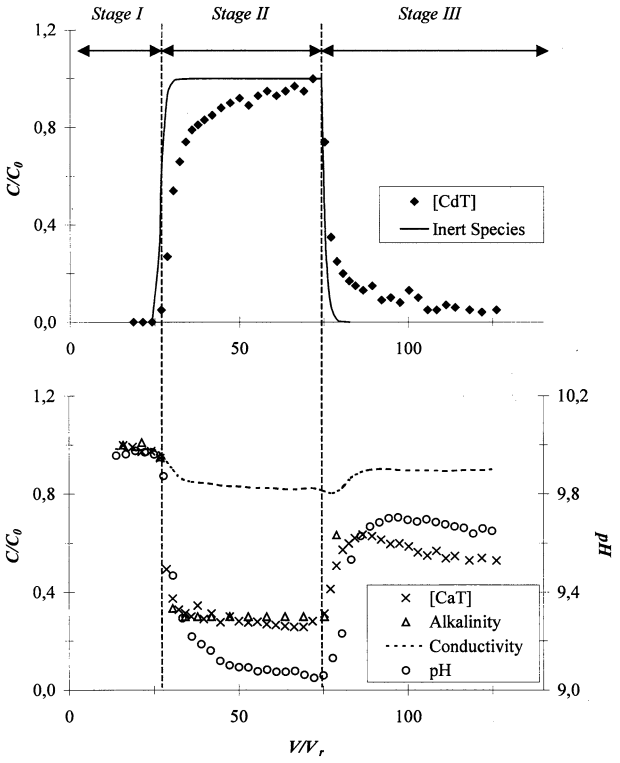


Fig. 3. Flow-through reactor experiment (*R14*, Table 4). The upper panel shows the dissolved $Cd^{2+}$ concentration measured in the outflow solution during the three stages of the experiment (defined in the text). The solid line corresponds to the theoretical BTC of an inert tracer. The lower panel displays the concentration of total dissolved $Ca^{2+}$, alkalinity, pH and conductivity in the outflow. The outflow $Cd^{2+}$ concentration is normalized to the inflow concentration during Stage II. The $Ca^{2+}$ concentration and the values of alkalinity and conductivity are normalized to their steady state values during Stage I. $V/V_r$ corresponds to the number of reactor volumes that have passed through the reactor.

that in the figure the X-axis corresponds to the number of reactor volumes ($V_r$) of solution that have passed through the reactor, the Y-axis to the concentration measured in the outflow, $C$, normalized to the input concentration, $C_o$, after the step increase. In this non-dimensional representation, the BTC of an inert solute is independent of the flow rate and input concentration.

Eqn. 12 provided an excellent fit to the conductivity tracer BTCs, over the entire range of flow rates tested. The presence of calcite in the reactor did not affect the conductivity BTCs. Similarly, the BTCs of dissolved cadmium for reactors without calcite matched Eqn. 12. Therefore, it can be assumed that aqueous concentrations were homogeneous within the reactor and equal to those measured in the outflow.

### 4.2. Cd-Calcite Interactions

When cadmium-free EqW and NEqW solutions were pumped through calcite-containing reactors (Stage I), outflow pH values were 8.0 ± 0.2 and 10.0 ± 0.2, respectively. The increase in pH between inflow and outflow in the NEqW solutions reflects calcite dissolution in the reactor, which consumes protons ($CaCO_{3(s)} + H^+ \rightleftarrows Ca^{2+} + HCO_3^-$). For a closed system, initially at equilibrium with atmospheric $CO_2$, pH reaches a value of ~10 when saturation with calcite is attained (Stumm and Morgan, 1981). If the system remains open to the atmosphere, the pH stabilizes around 8. The observed outflow pH values during Stage I in NEqW experiments therefore imply negligible exchange of $CO_2$ between the reactor and the atmosphere. Subsequent saturation state calculations assumed closed-system behavior of the reactor with respect to $CO_2$ partial pressure.

Cadmium breakthrough curves for $[Cd]_0 = 8.9\times10^{-9}$ mol $dm^{-3}$ in NEqW, at flow rates of 2.8, 1.4 and 0.3 $V_r$ $h^{-1}$, are presented in Figure 4. The BTCs are shifted down relative to that of the inert tracer, indicating retention of cadmium in the reactor. Experimental conditions, steady state solution compositions and amounts of cadmium removed (*Total* $Cd_{solid}$) from solution are presented in Tables 3 and 4. Also given here are the aqueous activities of calcium and cadmium at steady state, as well as the saturation indexes, SI = Log (ion activity product/$K_{so}$), with respect to calcite ($K_{calcite} = 10^{-9,3}$, experimental value) and otavite ($K_{otavite} = 10^{-12.1}$, Baes and Mesmer, 1976; Stipp et al., 1993), computed with the equilibrium speciation program MINTEQA2 (Allison et al., 1991).

In experiments run at the highest flow rate (2.8 $V_r$ $h^{-1}$), the cadmium concentration in the outflow approached the input concentration to within a few % during Stage II (e.g., Figs. 3, 4, 7). This was true even for experiments where the solution was oversaturated with respect to otavite. Hence, to a first approximation, the surface area between the observed BTC of

Table 3. Experimental conditions and results of cadmium flow-through experiments. EqW input solutions.[a]

| | *R34* | *R33* | *R27* | *R39* | *R18* | *R26* | *R25* | *R40* |
|---|---|---|---|---|---|---|---|---|
| Flow rate ($V_r$ $h^{-1}$) | 2.8 | 2.8 | 2.8 | 2.8 | 2.8 | 2.8 | 2.8 | 1.4 |
| $[Cd_T]_0$ | $4.5\ 10^{-9}$ | $8.9\ 10^{-9}$ | $4.5\ 10^{-8}$ | $6.2\ 10^{-8}$ | $8.9\ 10^{-8}$ | $2.2\ 10^{-7}$ | $4.5\ 10^{-7}$ | $8.9\ 10^{-7}$ |
| $(Cd^{2+})_{ss,(II)}$ | $1.7\ 10^{-9}$ | $3.4\ 10^{-9}$ | $1.7\ 10^{-8}$ | $2.4\ 10^{-8}$ | $3.4\ 10^{-8}$ | $8.6\ 10^{-8}$ | $1.7\ 10^{-7}$ | $2.9\ 10^{-7}$ |
| Total $Cd_{solid}$ | $5.1\ 10^{-8}$ | $7.9\ 10^{-8}$ | $1.9\ 10^{-7}$ | $5.4\ 10^{-7}$ | $1.1\ 10^{-6}$ | $1.4\ 10^{-6}$ | $2.5\ 10^{-6}$ | $1.3\ 10^{-5}$ |
| SI otavite | −2.36 | −2.06 | −1.36 | −1.21 | −1.06 | −0.66 | −0.36 | −0.13 |
| $R_{Cd}$ (mol $m^{-2}$ $h^{-1}$) | — | — | — | — | — | — | — | $1.9\ 10^{-7}$ |
| $[Cd_{ads}]_{max}$ | $5.1\ 10^{-8}$ | $7.9\ 10^{-8}$ | $1.9\ 10^{-7}$ | $5.4\ 10^{-7}$ | $1.1\ 10^{-6}$ | $1.4\ 10^{-6}$ | $2.5\ 10^{-6}$ | — |
| $[Cd_{ads}]_{min}$ | $3.6\ 10^{-8}$ | $5.6\ 10^{-8}$ | $1.3\ 10^{-7}$ | $4.0\ 10^{-7}$ | $7.6\ 10^{-6}$ | $1.1\ 10^{-6}$ | $2.2\ 10^{-6}$ | — |

[a] In all experiments, the initial amount of suspended calcite was 0.12 ± 0.01 g. Aqueous concentrations are given in mol $dm^{-3}$, sorbed concentrations in mol $m^{-2}$. $[Cd_{ads}]_{max}$ and $[Cd_{ads}]_{min}$ are the maximum and minimum estimates of adsorbed cadmium: $[Cd_{ads}]_{max}$ corresponds to the total uptake of dissolved $Cd^{2+}$ in experiments run at flow rate = 2.8 $V_r$ $h^{-1}$, $[Cd_{ads}]_{min}$ is corrected for the amount of Cd(II) that has diffused into the calcite lattice (Eqn. 17 in text). Duration of stage II: $t_{R40}$ = 25 h.

Table 4. Experimental conditions and results of cadmium flow-through experiments, NEqW input solutions.[a]

| | *R32* | *R24* | *R23* | *R31* | *R10* | *R14* | *R15* | *R19* | *R08* | *R37* | *R38* |
|---|---|---|---|---|---|---|---|---|---|---|---|
| Flow rate ($V_r$ $h^{-1}$) | 2.8 | 2.8 | 2.8 | 2.8 | 2.8 | 2.8 | 2.8 | 2.8 | 1.4 | 1.4 | 0.3 |
| $[Cd_T]_0$ | $2.2\ 10^{-9}$ | $4.5\ 10^{-9}$ | $8.9\ 10^{-9}$ | $8.9\ 10^{-8}$ | $4.5\ 10^{-7}$ | $8.9\ 10^{-7}$ | $1.8\ 10^{-6}$ | $4.4\ 10^{-6}$ | $8.9\ 10^{-7}$ | $8.9\ 10^{-9}$ | $8.9\ 10^{-9}$ |
| $(Cd^{2+})_{ss,\ (II)}$ | $4.8\ 10^{-10}$ | $6.0\ 10^{-10}$ | $1.7\ 10^{-9}$ | $1.7\ 10^{-8}$ | $1.2\ 10^{-7}$ | $2.9\ 10^{-7}$ | $5.9\ 10^{-7}$ | $1.4\ 10^{-6}$ | $1.6\ 10^{-7}$ | $9.0\ 10^{-10}$ | $<1.3\ 10^{-11}$ |
| $(Ca^{2+})_{ss,\ (II)}$ | $4.2\ 10^{-5}$ | $3.6\ 10^{-5}$ | $3.6\ 10^{-5}$ | $3.9\ 10^{-5}$ | $3.3\ 10^{-5}$ | $2.3\ 10^{-5}$ | $1.5\ 10^{-5}$ | $1.5\ 10^{-5}$ | $3.6\ 10^{-5}$ | $3.7\ 10^{-5}$ | $5.1\ 10^{-5}$ |
| $pH_{ss}$ ($\pm$0.2) | 9.7 | 9.7 | 9.6 | 9.4 | 9.1 | 8.9 | 8.7 | 8.7 | 9.5 | 9.8 | 10.0 |
| $Alk_{ss,\ (II)}$ | $1.7\ 10^{-4}$ | $1.7\ 10^{-4}$ | $1.7\ 10^{-4}$ | $1.2\ 10^{-4}$ | $0.9\ 10^{-4}$ | $0.6\ 10^{-4}$ | $0.5\ 10^{-4}$ | $0.5\ 10^{-4}$ | $1.0\ 10^{-4}$ | $1.7\ 10^{-4}$ | $2.0\ 10^{-4}$ |
| Total $Cd_{solid}$ | $6.4\ 10^{-8}$ | $1.4\ 10^{-7}$ | $1.7\ 10^{-7}$ | $1.2\ 10^{-6}$ | $8.6\ 10^{-6}$ | $8.8\ 10^{-6}$ | $9.9\ 10^{-6}$ | $1.1\ 10^{-5}$ | $1.7\ 10^{-5}$ | $3.0\ 10^{-7}$ | $3.8\ 10^{-7}$ |
| $SI_{calcite}$ ($\pm$0.2) | 0.2 | 0.1 | 0.1 | 0.1 | −0.3 | −0.8 | −1.4 | −1.5 | −0.3 | 0.2 | 0.4 |
| $SI_{otavite}$ ($\pm$0.2) | −2.0 | −1.9 | −1.5 | −0.4 | 0.1 | 0.1 | 0.0 | 0.3 | 0.2 | −1.7 | −3.4 |
| Desorption (%) | — | — | — | >87 | >74 | >80 | 100 | 100 | — | — | — |
| $R_{Cd}$ (mol $m^{-2}$ $h^{-1}$) | — | — | — | — | — | — | — | — | $2.4\ 10^{-7}$ | $4.2\ 10^{-9}$ | $2.6\ 10^{-9}$ |
| $[Cd_{ads}]_{max}$ | $6.4\ 10^{-8}$ | $1.4\ 10^{-7}$ | $1.7\ 10^{-7}$ | $1.2\ 10^{-6}$ | $8.6\ 10^{-6}$ | $8.8\ 10^{-6}$ | $9.9\ 10^{-6}$ | $1.1\ 10^{-5}$ | $8.7\ 10^{\times 6}$ | $1.5\ 10^{-7}$ | — |
| $[Cd_{ads}]_{min}$ | $3.5\ 10^{-8}$ | $8.2\ 10^{-8}$ | $1.2\ 10^{-7}$ | $8.7\ 10^{-7}$ | $6.2\ 10^{-6}$ | $6.4\ 10^{-6}$ | $7.7\ 10^{-6}$ | $9.8\ 10^{-6}$ | — | — | — |

[a] In all experiments, the initial amount of suspended calcite was 0.12 $\pm$ 0.01 g. Aqueous concentrations are given in mol $dm^{-3}$, sorbed concentrations in mol $m^{-2}$. $[Cd_{ads}]_{max}$ and $[Cd_{ads}]_{min}$ are the maximum and minimum estimates of adsorbed cadmium: $[Cd_{ads}]_{max}$ corresponds to the total uptake of dissolved $Cd^{2+}$ in experiments run at flow rate = 2.8 $V_r$ $h^{-1}$, $[Cd_{ads}]_{min}$ is corrected for the amount of Cd(II) that has diffused into the calcite lattice (Eqn. 17 in text). Duration of stage II: $t_{R08}$ = 40 h, $t_{R37}$ = 37 h.

aqueous cadmium and the inert tracer BTC provides an estimate of the amount of $Cd^{2+}$ adsorbed to the calcite grains. The adsorbed $Cd^{2+}$ surface concentrations calculated in this way are indicated as $[Cd_{ads}]_{max}$ in Tables 3 and 4. The adsorption isotherms measured at the highest flow rate in EqW and NeqW experiments are plotted in Figure 5.

In the experiments run at flow rates less than 2.8 $V_r$ $h^{-1}$, the steady state dissolved cadmium concentrations in the outflow never reached the input value (Fig. 4), implying a continued removal of dissolved $Cd^{2+}$ in the reactor. Stable outflow $Cd^{2+}$ concentrations and, thus, constant rates of "slow" uptake by calcite, were observed for durations of up to 15 h. Net rates of "slow" uptake calculated with Eqn. 13 are listed as $R_{Cd}$ in Tables 3 and 4.

A series of flow-through experiments was run to determine whether the solid-solution ratio and the analytical technique used to measure dissolved cadmium influenced the adsorption densities derived from cadmium BTCs. The three experiments were performed at a flow rate of 2.8 $V_r$ $h^{-1}$ with NEqW input solutions containing $[Cd]_0 = 8.9\times10^{-9}$ mol $dm^{-3}$. The calcite concentration in the reactor was varied and two different analytical techniques (ICP-MS and $\gamma$-counting) were used to measure dissolved cadmium in the outflow (Table 5). Within errors, the experiments yielded the same surface density of cadmium, 1.7 ($\pm$ 0.1) x$10^{-7}$ mol $m^{-2}$. The relative error on $Cd^{2+}$ surface densities presented in this paper was estimated to be $\pm$10%, with the largest contributions coming from the uncertainties associated with the mass and specific surface area of calcite added to the reactor.

Introduction of dissolved cadmium at the start of Stage II in NEqW experiments caused simultaneous decreases in outflow pH, alkalinity, calcium concentration and conductivity (Fig. 3), implying a decrease of the dissolution rate of calcite. Furthermore, the inhibitory effect on the dissolution kinetics (Table 6) increased with the amount of adsorbed cadmium (Fig. 6). In Figure 6, the relative inhibition is expressed as $(R_I - R_{II})/R_I$, where $R_I$ and $R_{II}$ are the steady state rates of dissolution measured before (Stage I) and after (Stage II) introducing

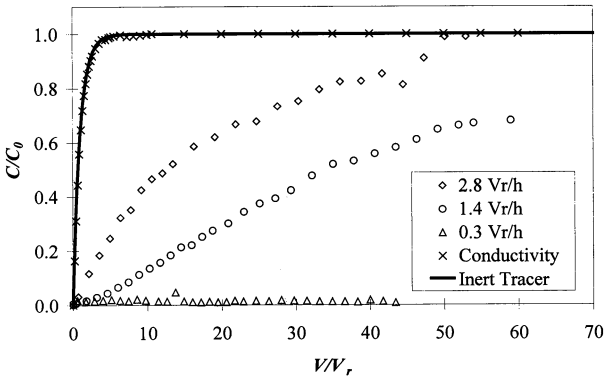


Fig. 4. Effect of flow rate on dissolved $Cd^{2+}$ breakthrough curves (BTCs) in the presence of calcite. Data plotted correspond to experiments *R23*, *R37* and *R38* in Table 4 ($[Cd]_0 = 8.9\times10^{-9}$ mol $dm^{-3}$). Also shown are the theoretical (full line) and experimental (crosses) inert tracer BTCs (conductivity). The horizontal axis gives the number of reactor volumes of input solution passed through the reactor. The origin coincides with the moment the initially $Cd^{2+}$-free input solution is switched to a $Cd^{2+}$-containing input solution (Stage II).

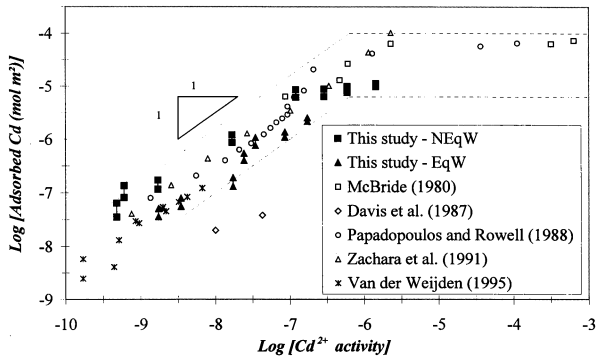


Fig. 5. Isotherms of $Cd^{2+}$ adsorption on calcite. Isotherms determined in flow-through reactor experiments with equilibrated (EqW) and non-equilibrated (NEqW) solutions in this study (data in Tables 3 and 4) are compared to those of previous studies (see Table 7). For each aqueous $Cd^{2+}$ activity in this study both the maximum and minimum estimate of the adsorbed $Cd^{2+}$ concentration is plotted (see text for discussion).

Table 5. Replicate $Cd^{2+}$ adsorption determinations in flow-through reactor experiments.[a]

| | Replicates | | |
|---|---|---|---|
| $m_{calcite}$ | 0.12 | 0.12 | 0.24 |
| Technique | ICP-MS | γ | γ |
| $Cd_{solid}$ | $1.78 \times 10^{-7}$ | $1.82 \times 10^{-7}$ | $1.58 \times 10^{-7}$ |

[a] Comparison of two analytical techniques for dissolved $Cd^{2+}$ measurements (gamma counting and ICP-MS), and effect of a doubling of the mass of calcite (in grams) suspended in the reactor. Experimental conditions: $[Cd]_0 = 8.9 \times 10^{-9}$ mol dm$^{-3}$; Q = 2.8 $V_r$ h$^{-1}$. Sorbed concentrations, $Cd_{solid}$, were derived from the measured $Cd^{2+}$ breakthrough curves and are expressed in mol m$^{-2}$.

cadmium to the reactor, respectively. The concentrations of adsorbed cadmium indicated on the figure were calculated from the adsorption isotherm for NEqW (Fig. 5) using the steady state aqueous Cd activity in the outflow during Stage II. The relative inhibition of calcite dissolution by adsorbed cadmium asymptotically approached 75–80% (Fig. 6). Therefore, calcite dissolution continued even when maximum surface coverage by $Cd^{2+}$ was reached.

Calcite dissolution rates were also determined after desorption of $Cd^{2+}$, that is, during Stage III. The results showed that, after removal of adsorbed $Cd^{2+}$ from the calcite particles, the dissolution rate remained below the initial value during Stage I (Table 6). This is particularly striking for experiments R15 and R19 where 100% of sorbed $Cd^{2+}$ was recovered during Stage III (Table 4). Despite the complete desorption of $Cd^{2+}$, the rate of dissolution of calcite was 30% lower than measured before the calcite surfaces had interacted with $Cd^{2+}$ ions.

### 4.3. Adsorption Isotherms

The cadmium adsorption isotherms differ for NEqW and EqW solutions: for the same free aqueous ($Cd^{2+}$) activity, the amount of cadmium removed by calcite is lower for EqW than for NEqW solution, as shown in Figure 5. The figure also compares the results of this study with those of McBride (1980), Davis et al. (1987), Papadopoulos and Rowell (1988), Zachara et al. (1991), and van der Weijden (1995). The adsorbed Cd concentrations are all given in units of mol m$^{-2}$ to account for differences in specific surface area of the calcite samples used. Experimental conditions of the various studies are summarized in Table 7.

Up to a $Cd^{2+}$ surface density of $\sim 10^{-5}$ mol m$^{-2}$, the results of previous studies mostly fall between the NEqW and EqW isotherms measured in this study. The general trend of the data defines a 1:1 slope on a log-log scale (Fig. 5). At surface densities $>10^{-5}$ mol m$^{-2}$, our data (especially in NEqW solution), as well as those of Papadopoulos and Rowell (1988) and McBride (1980), show a flattening of the isotherms. A likely explanation is that saturation of the surface adsorption sites is reached. The saturation value of $\sim 10^{-5}$ mol m$^{-2}$ observed in this study agrees with estimates of the density of lattice positions exposed on calcite surfaces (5 sites nm$^{-2}$, Möller and Sastri, 1974; Davis and Kent, 1990). The differences between the isotherms shown on Figure 5 are further analyzed in the Discussion section.

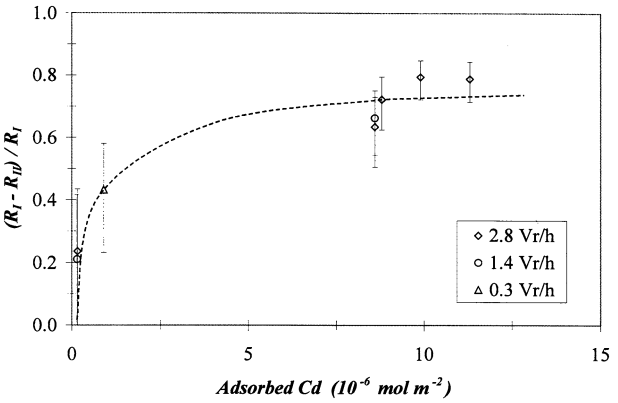


Fig. 6. Inhibition of calcite dissolution by adsorbed $Cd^{2+}$. The degree of inhibition is given as the relative drop of the steady state dissolution rate between Stages I and II. Dissolution rates were calculated with Eqn. 14.

The quantity of Cd desorbed from calcite was calculated by integrating the outflow $Cd^{2+}$ concentration from the beginning of Stage III until the end of the experiment. Table 4 reports the percentages of sorbed $Cd^{2+}$ that were remobilized by desorption in five experiments. In some cases, the outflow still had a significant dissolved $Cd^{2+}$ concentration at the end of the experiment. The corresponding desorption percentages in Table 4 are therefore identified as minimum estimates of the fraction of sorbed $Cd^{2+}$ that could be recovered from the calcite particles.

Results of desorption experiments showed that 80 to 100% of $Cd^{2+}$ removed from solution by "fast" adsorption was recovered after switching to Cd-free NEqW solutions (Table 4). During desorption, it took on the order of 10–20 h to reach steady state at a flow rate of 2.8 $V_r$ h$^{-1}$. Under similar conditions, steady state is reached within 3 h for an inert species. In the experiments at flow rate 2.8 $V_r$ h$^{-1}$, no effect of the contact time between calcite and cadmium-containing solutions on cadmium desorption was observed in the concentration range

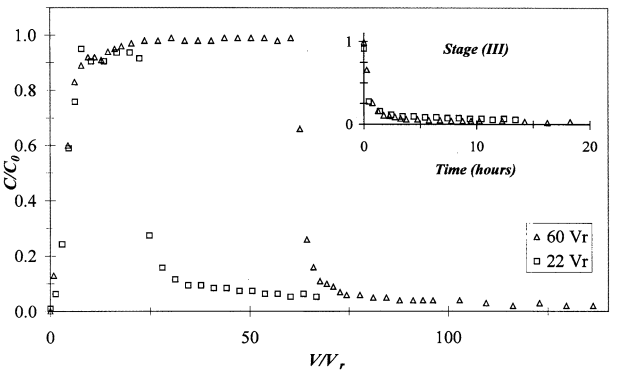


Fig. 7. Comparison of normalized $Cd^{2+}$ outflow concentrations during Stages II and III, in two experiments where the duration of Stage II was equivalent to 22 and 60 $V_r$, respectively. Input solutions contained $4.4 \times 10^{-6}$ mol dm$^{-3}$ of dissolved $Cd^{2+}$ and were supplied at a constant flow rate (2.8 $V_r$ h$^{-1}$) in both experiments. The origin of time in the insert corresponds to the beginning of Stage III for both experiments. The results show no effect of the duration of Stage II on the $Cd^{2+}$ desorption curves.

Table 6. Inhibitory effect of $Cd^{2+}$ sorption on calcite dissolution kinetics. $R_i$ (i = I, II, III) represent the rates of calcite dissolution during the successive stages of the flow-through experiments (see Fig. 3).

| | *R23* | *R31* | *R10* | *R14* | *R15* | *R19* | *R08* | *R37* | *R38* |
|---|---|---|---|---|---|---|---|---|---|
| $(R_I - R_{II})/R_I$ | 0.24 | 0.41 | 0.63 | 0.72 | 0.80 | 0.79 | 0.66 | 0.21 | 0.43 |
| $(R_I - R_{III})/R_I$ | — | — | 0.31 | 0.46 | 0.31 | 0.27 | — | — | — |

$4.45\times10^{-7}$ to $4.45\times10^{-6}$ mol $dm^{-3}$. This is illustrated in Figure 7 where identical desorption curves are observed whether 22 or 60 reactor volumes ($V_r$) of Cd-containing solution passed through the reactor during Stage II.

### 4.4. Slow Aqueous $Cd^{2+}$ Uptake

For the same input concentration of $Cd^{2+}$, $[Cd]_{ss}/[Cd]_0$ was equal to 1.0, 0.65, and 0.05 at flow rates of 2.8, 1.4 and 0.3 $V_r$ $h^{-1}$, respectively (Fig. 4). Thus, for water residence times greater than 0.5 h, uptake processes other than equilibrium adsorption had a pronounced effect on the outflow concentrations of aqueous cadmium. "Slow" uptake of cadmium occurred even for total Cd uptake significantly below saturation of the surface sites and for solutions undersaturated with respect to otavite.

The rates of "slow" Cd uptake by calcite, $R_{Cd}$, were calculated with Eqn. 13 for experiments *R08*, *R37*, *R38* and *R40* (Tables 3 and 4). The rates are order-of-magnitude higher than those of Davis et al. (1987) who reported a rate of "slow" uptake of $7.5\times10^{-11}$ mol $m^{-2}$ $h^{-1}$. In the experiments with flow rates $<2.8$ $V_r$ $h^{-1}$, steady state conditions during Stage II and, thus, constant rates of "slow" cadmium uptake were maintained for periods of up to 15 h. The slow uptake rates, however, were found to depend on the concentrations of adsorbed cadmium derived from the isotherms: the higher the surface density of adsorbed cadmium, the higher the rate of "slow" uptake.

The dependence of the rate of "slow' cadmium uptake on the concentration of adsorbed $Cd^{2+}$ was fitted to a first order expression:

$$R_{Cd} = k\,[Cd_{ads}] \qquad (15)$$

The apparent first order rate constant, $k$, derived from the data of experiments *R08*, *R37*, *R38* and *R40*, was 0.030 ($\pm$0.005) $h^{-1}$. The characteristic time scale of "slow" $Cd^{2+}$ incorporation was therefore on the order of 30 h, compared to the characteristic time scale of "fast" $Cd^{2+}$ adsorption of less than 0.5 h. Experiments with EqW and NEqW input solutions defined a single trend, suggesting that the rate of incorporation of $Cd^{2+}$ was not affected by dissolution of the calcite grains.

## 5. DISCUSSION

### 5.1. Adsorption Isotherms

At equal free aqueous $Cd^{2+}$ activities, 40–50% more $Cd^{2+}$ ions are adsorbed in NEqW than EqW solutions (Fig. 5). Previous studies have shown that pH and the presence of divalent cations, such as $Ca^{2+}$ and $Mg^{2+}$, influence cation adsorption on calcite. In particular, calcium competes with adsorption of $Co^{2+}$ (Kornicker et al., 1985), $Zn^{2+}$ (Zachara et al., 1988) and $Cd^{2+}$ (Franklin and Morse, 1983; Davis et al., 1987; Zachara et al., 1991) on calcite.

The cation exchange model (Eqns. 2 and 3) is the simplest model describing the effect of $Ca^{2+}$ ions on $Cd^{2+}$ adsorption to calcite surfaces. The model was fitted to the ($Cd^{2+}$) and ($Ca^{2+}$) free ion activity values listed in Tables 3 and 4, yielding a maximum $Cd^{2+}$ adsorption density, $X_T$, of $1.1\times10^{-5}$ mol $m^{-2}$. As can be seen in Figure 8, the Ca-Cd exchange model reproduces the difference between the NEqW and EqW isotherms. The fit to the data yields a Log $c_{K_{ex}}$ value of 2.5 (Eqn. 3 with $n = 1$). The value of the equilibrium exchange constant depends on the value of $X_T$. If a cation surface site density of 5 atoms Ca per $nm^2$ is used (Möller and Sastri, 1974), the corresponding $X_T$ value equals $8\times10^{-6}$ mol $m^{-2}$ and the best fit to the observed isotherms gives Log $c_{K_{ex}} = 2.7$. In this case, however, the model slightly underestimates the maximum adsorbed cadmium concentrations. The conditional stability con-

Table 7. Comparison of experimental conditions in this and previous studies of $Cd^{2+}$ sorption to calcite.[a]

| | NEqW | EqW | McBride (1980) | Davis et al. (1987) | Papadopoulos and Rowell (1988) | Zachara et al. (1991) | van der Weijden (1995) |
|---|---|---|---|---|---|---|---|
| T (°C) | 25 ± 0.5 | | 23 ± 2 | 25 | 25 ± 1 | 25 | 20 ± 2 |
| Input solution | P.W. | Eq. | P.W. | Eq. | Eq. | Eq. | Eq. |
| Electrolyte | NaCl | | — | AGW | $Ca(NO_3)_2$ | — | NaCl |
| Log $Pco_2$ | variable | −3.5 | −3.5 | −3.5 to 1 | −3.5 | −3.5 | −3.5 |
| pH | 8.9–9.8 | 7.9–8.2 | 6.5–8.3 | 6.0–8.25 | 6.4–8.3 | 7.4 | 7.9 |
| I (mol $dm^{-3}$) | 0.01 | | — | variable | variable | 0.1 | 0.1–0.7 |
| SA ($m^2$ $g^{-1}$) | 0.28 | | 0.49 | 0.50 | 0.15 | 0.20 | 0.13 |
| Particle size ($\mu$m) | 100–140 | | — | 2–4 | — | 9 | 10–100 |
| Solid/solution (g $dm^{-3}$) | 3.33 | | 8.0 | — | 80 | 25 | 4.94 |
| Contact time (h) | 5–20 | | 24 | 24 | 72 | 24–36 | 49 |

[a] P.W. = pure water; Eq. = equilibrated water; AGW = artificial ground water. In contrast to this study, all previous studies were conducted in batch reactors.

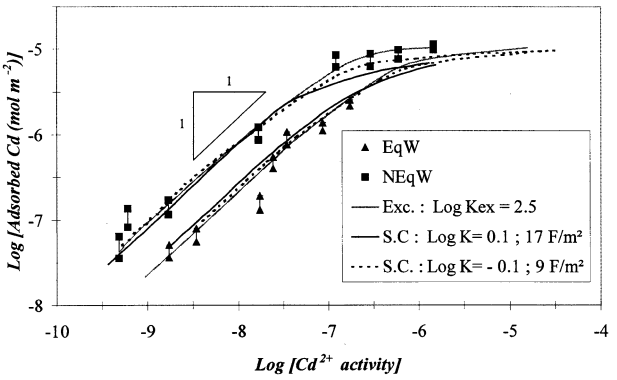


Fig. 8. Adsorption models. Minimum and maximum estimates of adsorbed $Cd^{2+}$ concentrations are plotted for flow-through reactor experiments using EqW and NEqW input solutions. Lines correspond to fits of the Cd-Ca exchange (Exc.) and surface complexation (S.C.) models to the data. For the latter model, fits for two different electric double layer capacitance values are shown. See text for complete discussion.

stants derived here are smaller, although of the same order of magnitude, as previously reported values (Log $c_{K_{ex}} = 3.02$–3.03, Zachara et al., 1991; 3.02–3.12, van der Weijden, 1995) and $D$ values (log $D = 3.18$, Davis et al., 1987; 3.5, Papadopoulos and Rowell, 1988).

The cation-exchange model only describes the competition between $Ca^{2+}$ and $Cd^{2+}$ for the same population of surface sites. In addition to competition by $Ca^{2+}$, the surface complexation model accounts for effects of pH and $P_{CO2}$ on $Cd^{2+}$ binding to calcite surfaces. Application of the surface complexation model predicts that during Stage I the calcite surfaces are dominated by $>CO_3^-$, $>CO_3Ca^+$ and $>CaCO_3^-$ species, both in NEqW and EqW solutions. With the default values for the surface site density, $X_T = 1.1\times10^{-5}$ mol $m^{-2}$, and the capacitance of the electrical double layer, $\kappa = 17$ F $m^{-2}$, fitting of the isotherms gives a stability constant for the surface complex $>CO_3Cd^+$ (Eqn. 10) of Log $K_{(10)} = 0.1$. Inclusion of reaction 11 does not improve the fit to the data and no value for Log $K_{(11)}$ was therefore determined. The EqW isotherm is well reproduced, while for NEqW a reasonable fit is found for aqueous $Cd^{2+}$ activities below $10^{-7}$ (Fig. 8). At higher aqueous activities, adsorbed concentrations in NEqW are underestimated. Decreasing the capacitance improves the agreement between model and data without a large change in Log $K_{(10)}$ (see data fit for $\kappa = 9$ F $m^{-2}$ and Log $K_{(10)} = -0.1$ in Figure 8.

With the necessary parameter adjustments, both adsorption models provide equally good fits to the observed isotherms (Fig. 8). Analysis of the chemical structure of the calcite surface predicted by the surface complexation model speciation reveals why this is so. In experiments both with NEqW and EqW input solutions, the dominant adsorption sites for both $Ca^{2+}$ and $Cd^{2+}$ are surface carbonate groups. Only at pH > 10 do surface hydroxyl sites ($>CaOH^0$) become available for cation adsorption. Therefore, within the framework of the surface complexation model, reactions (9) and (10) account for the adsorption of $Ca^{2+}$ and $Cd^{2+}$ on calcite surfaces over the range of conditions encountered in the flow-through experiments. Combined, these reactions give

$$>CO_3Ca^+ + Cd^{2+} \Leftrightarrow >CO_3Cd^+ + Ca^{2+} \qquad (16)$$

which is formally equivalent to the cation surface exchange reaction 2. Based on the intrinsic stability constants for reactions (9) and (10), Log $K_{(16)}$ is calculated to be in the range 2.7–2.9. Thus, as expected, $K_{(16)}$ is of the same order of magnitude as $c_{K_{ex}}$.

The intrinsic surface stability constant for the adsorption of $Ca^{2+}$ ions to carbonate surface sites, i.e., reaction (9) listed in Table 1 (Log $K_{(9)} = -2.8$), is not an experimentally-determined value, but a rough estimate derived from the formation constant of the dissolved complex $CaHCO_3^+$ (see Van Cappellen et al., 1993, for complete discussion). In recent studies, Pokrovsky et al. (1998) and Fenter et al. (2000) have proposed higher ($-1.7$) and lower ($< -4.4$) values for log $K_{(9)}$. Variations in log $K_{(9)}$ affect the value of log $K_{(10)}$ obtained from fitting the $Cd^{2+}$ adsorption isotherms, but not that of log $K_{(16)}$. Thus, while considerable uncertainty remains concerning the absolute values of the stability constants for the formation of the $>CO_3Cd^+$ and $>CO_3Ca^+$ surface complexes, their relative magnitudes appear well constrained.

In principle, the surface complexation model provides a more general description of carbonate mineral-aqueous solution interactions, compared to the cation exchange model. It offers a single theoretical framework in which mineral dissolution and precipitation kinetics, surface charge development and sorption properties are explained in terms of reactions between surface hydration species ($>CaOH^0$ and $>CO_3H^0$) and aqueous constituents (Van Cappellen et al., 1993). The existence of $>CaOH^0$ and $>CO_3H^0$ surface sites at the termination of the calcite lattice is supported by observations using high-resolution surface observation techniques (e.g., Stipp and Hochella, 1991; Pokrovsky et al., 1998; Fenter et al., 2000). As shown here, the simpler cation exchange model represents a special case of the surface complexation model of the calcite-aqueous solution interface.

Values of the exchange constant $c_{K_{ex}}$, $D$ or $K_{(16)}$ derived from the data presented here are lower than found in the literature. Furthermore, the maximum adsorption density observed in this study is significantly lower than reported by McBride (1980), and Zachara et al. (1991) (Fig. 5). One reason for the discrepancies may be that previous $Cd^{2+}$ sorption studies were carried out in batch reactors. Measurements of $Cd^{2+}$ uptake by calcite in batch systems include contributions of both "fast" and "slow" uptake processes, as recognized by Papadopoulos and Rowell (1988). These authors separated their $Cd^{2+}$ uptake data into two regimes, one corresponding to the progressive saturation of available surface sites, the other to surface precipitation which they assumed starts only after monolayer surface coverage by $Cd^{2+}$ has been reached. The kinetic $Cd^{2+}$ uptake data presented here, however, show that "slow" incorporation begins well below $Cd^{2+}$ surface saturation. This is in agreement with the observations of Davis et al. (1987) and Stipp et al. (1992). The former authors found that uptake processes other than reversible adsorption occur even at less than 1% monolayer surface coverage, while Stipp et al. (1992) observed the disappearance of cadmium adsorbed at the surface, as a result of diffusion into the calcite crystal, at surface coverages below 25%.

According to the experimental results presented here, the

effect of "slow" uptake on total aqueous $Cd^{2+}$ removal by calcite becomes important at reaction times exceeding 0.5 h. Batch sorption experiments are typically run for much longer times (Table 7). Hence, the variability of isotherms measured previously in solutions equilibrated with calcite (Fig. 6) may in part reflect variable contributions of "slow" uptake processes among the different studies.

The flow-through experiments conducted in this study ran for 5 to 20 h. Some $Cd^{2+}$ uptake by calcite is therefore due to "slow" incorporation, even in the high flow rate (2.8 $V_r$ $h^{-1}$) regime. The maximum contribution of "slow" uptake to total removal of aqueous $Cd^{2+}$, can be calculated using a constant rate of incorporation, $R_{Cd} = k[Cd_{ads}]_{min}$, during the time necessary to reach steady state conditions in Stage II, $t_{II}$. The corresponding minimum estimate of the concentration of truly adsorbed $Cd^{2+}$, $[Cd_{ads}]_{min}$, is related to the maximum estimate $[Cd_{ads}]_{max}$ (Tables 3 and 4) by

$$[Cd_{ads}]_{max} = [Cd_{ads}]_{min}(1 + kt_{II}) \quad (17)$$

The minimum estimates of the concentrations of adsorbed $Cd^{2+}$ are listed in Tables 3 and 4. Both the maximum and minimum adsorbed concentrations are shown on Figures 5 and 8. It can be seen that "slow" uptake mainly affects the estimated adsorbed surface densities of $Cd^{2+}$ at the lowest dissolved $Cd^{2+}$ levels.

Based on the previous discussion, we propose that the smaller exchange constants (as $c_{K_{ex}}$ or $K_{(16)}$) and saturation site densities found using the flow-through reactor technique provide a more accurate representation of "true" surface adsorption of $Cd^{2+}$ on calcite than values derived from batch experiments.

### 5.2. Desorption

Desorption of $Cd^{2+}$ from calcite is characterized by an initial rapid release of $Cd^{2+}$ ions, followed by the persistence of non-zero outflow concentrations over relatively long times (Figs. 3 and 7). Tailing of the desorption curves could correspond to the release of $Cd^{2+}$ removed during "slow" uptake. This explanation, however, does not agree with the lack of dependence of the desorption tails on the duration of the preceding sorption period (Fig. 7). Furthermore, the amounts of $Cd^{2+}$ released during tailing exceed the maximum estimated concentrations of $Cd^{2+}$ fixed by "slow" uptake. Alternatively, the observed tailing could reflect the existence of several surface coordination environments for $Cd^{2+}$. Differences in bonding could result in differences in desorption kinetics. Further kinetic experiments, as well as spectroscopic observations, will be needed to determine the mechanism(s) responsible for the observed desorption behavior.

### 5.3. Slow $Cd^{2+}$ Uptake

Cadmium solid-state diffusion into the calcite lattice from adsorbed positions has been proposed as a mechanism leading to otavite–calcite solid-solution formation (Stipp et al., 1992). Assuming that the thickness of the adsorbed layer and the diffusion jump distance are both equal to the thickness of a $CaCO_3$ unit cell along the cleavage plane ($d = 3.2$ Å; Liang and Bear, 1997), and assuming that the rate constant of "slow" uptake ($k = 0.03\ h^{-1}$) can be equated to the jump frequency of $Cd^{2+}$ ions from surface sites to underlying lattice sites, a corresponding solid-state diffusion coefficient, $D_s$, at 25°C can be calculated as $D_s = k(d)^2$ (Lasaga, 1998). The calculation yields $D_s = 8.5\ (\pm 1.4)\ x10^{-21}\ cm^2\ s^{-1}$.

The value of $D_s$ calculated here falls in between values of solid state diffusion coefficients at 25°C of $^{45}Ca$ in calcite ($8\times10^{-20}\ cm^2\ s^{-1}$; Lahav and Bolt, 1964) and alkali cations (Rb, Cs, Sr) in the hydrated surface layers of silicate glasses ($\leq10^{-21}\ cm^2\ s^{-1}$; White and Yee, 1986). Thus, in terms of magnitude, the kinetics of the "slow" uptake process are compatible with diffusion of adsorbed $Cd^{2+}$ ions into the calcite lattice. The value of $D_s$ is also consistent with the changes in $Cd^{2+}$ surface concentration on calcite observed by Stipp et al. (1992).

According to Einstein's equation, $z = \sqrt{D_s t}$, where $x$ and $t$ are distance and time, $Cd^{2+}$ should not have diffused beyond the first surface $CaCO_3$ monolayer during the 5–20 h of Stage II of the flow-through experiments. The amount of $Cd^{2+}$ needed to form a monolayer of otavite–calcite solid solution in equilibrium with a given experimental solution can be determined with Eqn. 1, using the aqueous $Ca^{2+}$ and $Cd^{2+}$ activities (Tables 2–4), and assuming a total number of cation positions of $1.1\times10^{-5}\ mol\ m^{-2}$ in a $CaCO_3$ monolayer. The measured kinetics of "slow" uptake (Eqn. 15) then predict that it would take between 30 and 400 h to produce a monolayer of solid solution at equilibrium with the solution, depending on the dissolved $Cd^{2+}$ level. If the slow uptake process indeed corresponds to $Cd^{2+}$ diffusion into the surface lattice, then these times are absolute minimum estimates, because (1) for times >30 h $Cd^{2+}$ will have penetrated beyond the outermost monolayer, and (2) the rate of diffusion will slow down as $Cd^{2+}$ starts building up in the mineral surface lattice. From these considerations, it appears that only the initial stage of solid-solution formation may have been reached during the experiments.

### 5.3. Calcite Dissolution

Cadmium adsorption has an instantaneous inhibitory effect on calcite dissolution (Fig. 3). At only one fifth of the maximum adsorption density, adsorbed $Cd^{2+}$ ions reduce the dissolution rate of calcite by 50% (Fig. 6). This suggests that $Cd^{2+}$ preferentially attaches to reactive dissolution sites, e.g., kink and edge sites (Reeder, 1996; Schosseler et al., 1999), leading to a competition between adsorption and dissolution processes. When $Cd^{2+}$ adsorption reaches its maximum coverage ($X_T = 1.1\times10^{-5}\ mol\ m^{-2}$), however, dissolution still proceeds at a rate equal to 25% of its initial value under Cd-free conditions. This non-zero rate is too fast to be explained by release of $Ca^{2+}$ ions coupled to "slow" incorporation of $Cd^{2+}$ into the lattice by diffusion. Thus, it would appear that a fraction of dissolution sites at the calcite surface remains active in the presence of $Cd^{2+}$. A complete understanding of the observed effect of $Cd^{2+}$ adsorption on calcite dissolution will require a detailed characterization of the kinetic and structural properties of surface sites at the calcite mineral-aqueous solution interface.

Desorption of $Cd^{2+}$ does not restore the calcite dissolution rate to its preadsorption value, even when desorption is 100% complete (Tables 3, 4, and 6). Previous studies have demon-

strated the highly dynamic nature of calcite surfaces and have documented significant modifications of the surface structure upon interaction with solute species (e.g., Hillner et al., 1992; Dove and Hochella, 1993; Reeder, 1996; Liang and Baer, 1997; Teng et al., 1998, 1999; Fenter et al., 2000). The results presented here confirm that interaction with $Cd^{2+}$ changes the dissolution kinetics of calcite but, in addition, they suggest that the calcite surfaces retain a "memory" of the adsorbed $Cd^{2+}$ ions after they return to solution.

The flow-through reactor study shows that calcite crystals present in sediments, soils and aquifers have the potential to immobilize $Cd^{2+}$ via adsorption and bulk incorporation. Equally important, the results show that interactions with $Cd^{2+}$ have profound effects on the reactivity of calcite.

## 6. CONCLUSIONS

The interactions of $Cd^{2+}$ ions with calcite surfaces were investigated in NaCl solutions at 25°C using stirred flow through reactors. By varying the solution residence time in the reactor, $Cd^{2+}$ uptake due to "fast" surface adsorption and to "slow" bulk incorporation could be measured separately. The flow-through technique also allowed us to monitor the effect of cadmium uptake on the dissolution kinetics of calcite. The following are the main conclusions of this study.

1. For water residence times less than 0.5 h, the breakthrough curves of dissolved cadmium are mainly affected by adsorption of $Cd^{2+}$ at the calcite-aqueous solution interface. Cadmium adsorption is lower in EqW than in NEqW solutions. For the range of solution compositions encountered in this study, the difference between EqW and NEqW isotherms is attributed to competition of $Ca^{2+}$ ions with $Cd^{2+}$ ions for surface carbonate ligands.
2. The $Cd^{2+}$-$Ca^{2+}$ surface exchange constant (Log ${}^{c}K_{ex} = 2.5$) and the maximum $Cd^{2+}$ adsorption density on calcite ($X_T = 1.1\times10^{-5}$ mol $m^{-2}$) determined in this study are lower than reported in the literature. This may reflect the fact that previous isotherms were measured in batch reactors and may have been affected to a larger degree by uptake processes other than true adsorption.
3. Rates of slow $Cd^{2+}$ uptake remain constant for periods of up to 15 h and are proportional to the surface density of adsorbed $Cd^{2+}$ ions. The diffusion coefficient describing transfer of $Cd^{2+}$ ions from the surface into the solid phase ($8.5\times10^{-21}$ $cm^2$ $s^{-1}$) implies that, for the duration of the experiments (5–20 h), migration of $Cd^{2+}$ cations into the lattice is limited to the outermost few Å.
4. The flow-through experiments confirm the continuum between adsorption and slow uptake when $Cd^{2+}$ containing solutions are in contact with calcite surfaces. The kinetic data for slow uptake are consistent with migration of surface-bound $Cd^{2+}$ into the calcite lattice, leading to the progressive formation of a $CaCO_3$-$CdCO_3$ solid solution in the near-surface of the crystals.
5. Adsorption of $Cd^{2+}$ inhibits the dissolution of calcite crystals. The degree of inhibition increases with the surface density of adsorbed $Cd^{2+}$ and reaches a maximum of ~75% when maximum $Cd^{2+}$ adsorption coverage is reached. This indicates that a subset of the dissolution sites remains active in the presence of adsorbed $Cd^{2+}$ ions. Upon desorption of $Cd^{2+}$, the calcite dissolution rate increases again, but does not return to its initial value even for 100% desorption. The nature of this "hysteresis" effect is presently unknown.

*Acknowledgments*—The manuscript benefited from the insightful and thorough comments of Susan Stipp, an anonymous Journal reviewer and the Associate Editor, Michael Machesky. This research has been financially supported by the French Atomic Energy Agency (CEA-PhD fellowship to AMG) and by the Netherlands Organisation of Scientific Research (NWO-Van Gogh Fellowship to PVC).

*Associate editor:* M. Machesky

## REFERENCES

Allison J. D., Brown D. S., and Novo-Gradac K. J. (1991) *MINTEQA2/PRODEFA2, A Geochemical Assessment Model for Environmental Systems: Version 3.0 User's Manual*.U.S. Environmental Protection Agency.

Arakaki T. and Mucci A. (1995) A continuous and mechanistic representation of calcite reaction-controlled kinetics in dilute solutions at 25°C and 1 atm total pressure. *Aquat. Geochem.* **1,** 105–130.

Baes C. F. and Mesmer R. E. (1976) *The Hydrolysis of Cations.* Wiley.

Busenberg E. and Plummer L. N. (1989) Thermodynamics of magnesian calcite solid-solutions at 25°C and 1 atm total pressure. *Geochim. Cosmochim. Acta* **53,** 1189–1208.

Chang L. L. Y. and Brice W.R. (1971) Subsolidus phase relations in the system calcium carbonate–cadmium carbonate. *Am. Mineral.* **56,** 338–341.

Charlet L. (1994) Reactions at the mineral–water interface. In *Chemistry of Aquatic Systems: Local and Global Perspectives* (eds. G. Bidoglio and W. Stumm), pp. 273–305. Kluwer.

Chiarello R. P. and Sturchio N. C. (1994) Epitaxial growth of otavite on calcite observed in situ by synchrotron X-ray scattering. *Geochim. Cosmochim. Acta* **58,** 5633–5638.

Chiarello R. P., Sturchio N. C., Grace J. D., Geissbuhler P., Sorensen L. B., Cheng L., and Xu S. (1997) Otavite–calcite solid-solution formation at the calcite-water interface studied in situ by synchrotron X-ray scattering. *Geochim. Cosmochim. Acta* **61,** 1467–1474.

Davis J. A., Fuller C. C., and Cook A. D. (1987) A model for trace metal sorption processes at the calcite surface: Adsorption of $Cd^{2+}$ and subsequent solid solution formation. *Geochim. Cosmochim. Acta* **51,** 1477–1490.

Davis J. A. and Kent D. B. (1990) Surface complexation modeling in aqueous geochemistry. In *Mineral–Water Interface Geochemistry* (eds. M. F. Hochella and A. F. White), pp. 177–260. Reviews in Mineralogy 23. American Mineralogical Society.

Dove P. M. and Hochella M. F. Jr. (1993) Calcite precipitation mechanisms and inhibition by orthophosphates: In situ observations by Scanning Force Microscopy. *Geochim. Cosmochim. Acta* **57,** 705–714.

Fenter P., Geissbühler P., DiMasi E., Srajer G., Sorensen L. B., and Sturchio N. C. (2000) Surface speciation of calcite observed in situ by high-resolution X-ray reflectivity. *Geochim. Cosmochim. Acta* **64,** 1221–1228.

Fouillac C. and Criaud A. (1984) Carbonate and bicarbonate trace metal complexes: Critical reevaluation of stability constants. *Geochemical J.* **18,** 297–303.

Franklin M. L. and Morse J. W. (1983) The interaction of manganese(II) with the surface of calcite in dilute solutions and seawater. *Mar. Chem.* **12,** 241–254.

Grolimund D., Borkovec M., Federer P., and Sticher H. (1995) Measurement of sorption isotherms with flow-through reactors. *Environ. Sci. Technol.* **29,** 2371–2321.

Hillner P. E., Gratz A. J., Manne S., and Hansma P. K. (1992) Atomic-scale imaging of calcite growth and dissolution in real time. *Geology* **20,** 359–362.

Königsberger E., Hausner R., and Gamsjäger H. (1991) Solid-solution phase equilibria in aqueous solution. V: The system $CdCO_3$-$CaCO_3$-$CO_2$-$H_2O$. *Geochim. Cosmochim. Acta* **55,** 3505–3514.

Kornicker W. A., Morse J. W., and Damasceno R. N. (1985) The chemistry of $Co^{2+}$ interaction with calcite and aragonite surfaces. *Chem. Geol.* **53,** 229–236.

Lahav N. and Bolt G. H. (1964) Self-diffusion of $^{45}Ca$ into certain carbonates. *Soil Sci.* **93,** 293–299.
Lasaga A. C. (1998) *Kinetic Theory in the Earth Sciences.* Princeton University Press.
Liang Y. and Baer D. R. (1997) Anisotropic dissolution at the $CaCO_3$ (1*0*1*4*)–water interface. *Surface Sci.* **373,** 275–287.
Lorens R. B. (1981) Sr, Cd, Mn and Co distribution coefficients in calcite as a function of calcite precipitation rate. *Geochim. Cosmochim. Acta* **45,** 553–561.
McBride M. B. (1980) Chemisorption of $Cd^{2+}$ on calcite surfaces. *Soil Sci. Soc. Am. J.* **44,** 26–28.
Möller P. and Sastri C. S. (1974) Estimation of the number of surface layers of calcite involved in $^{45}Ca$-Ca isotopic exchange with solution. *Z Phys. K. Chem. Folge.* **89,** 80–87.
Mucci A. (1986) Growth kinetics and composition of magnesian calcite overgrowths precipitated from seawater: Quantitative influence of orthophophate ions. *Geochim. Cosmochim. Acta* **50,** 2255–2265.
Nagy K. L. and Lasaga A. C. (1992) Dissolution and precipitation kinetics of gibbsite at 80°C and pH 3: The dependence on solution saturation state. *Geochim. Cosmochim. Acta* **56,** 3093–3111.
Nilsson Ö. and Sternbeck J. (1999) A mechanistic model for calcite crystal growth using surface speciation. *Geochim. Cosmochim. Acta* **63,** 217–225.
Papadopoulos P. and Rowell D. L. (1988) The reaction of cadmium with calcium carbonate surfaces. *J. Soil Sci.* **39,** 23–36.
Pokrovsky O. S., Schott J., Thomas F., and Mielczarski J. (1998) Surface speciation of Ca and Mg carbonate minerals in aqueous solutions: A combined potentiometric, electrokinetic, and DRIFT surface spectroscopy approach. *Min. Mag.* **62A,** 1196–1197.
Pokrovsky O. S. and Schott J. (1999) Processes at the magnesium-bearing carbonates/solution interface II. Kinetics and mechanism of magnesite dissolution. *Geochim. Cosmochim. Acta* **63,** 881–897.
Pokrovsky O. S., Schott J., and Thomas F. (1999) Processes at the magnesium-bearing carbonates/solution interface I. A surface speciation model for magnesite. *Geochim. Cosmochim. Acta* **63,** 863–880.
Reeder R. J. (1996) Interaction of divalent cobalt, zinc, cadmium, and barium with the calcite surface during layer growth. *Geochim. Cosmochim. Acta* **60,** 1543–1552.
Scheidegger A. M. and Sparks D. L. (1996) A critical assessment of sorption-desorption mechanisms at the soil mineral/water interface. *Soil Sci.* **161,** 813–831.
Schosseler P. M., Wehrli B., and Schweiger A. (1999) Uptake of $Cu^{2+}$ by the carbonates vaterite and calcite as studied by continuous wave (CW) and pulse electron paramagnetic resonance. *Geochim. Cosmochim. Acta* **63,** 1955–1967.
Sposito G. A. (1986) Distinguishing adsorption from surface precipitation. In *Geochemical Processes at Mineral Surfaces* (eds. J. A. Davis and K. H. Hayes), pp. 217–228, Symposium Series 323. American Chemical Society.
Stipp S. L. and Hochella M. F. (1991) Structure and bounding environments at the calcite surface as observed with X-ray photoelectron spectroscopy (XPS) and low energy electron diffraction (LEED). *Geochim. Cosmochim. Acta* **55,** 1723–1736.
Stipp S. L., Hochella M. F., Parks G. A., and Leckie J. O. (1992) $Cd^{2+}$ uptake by calcite, solid-state diffusion, and the formation of solid-solution: Interface processes observed with near-surface sensitive techniques (XPS, LEED, and AES). *Geochim. Cosmochim. Acta* **56,** 1941–1954.
Stipp S. L., Parks G. A., Nordstrom D. K., and Leckie J. O. (1993) Solubility-product constant and thermodynamic properties for synthetic otavite, $CdCO_3$(s), and aqueous association constants for the Cd (II)-$CO_2$-$H_2O$ system. *Geochim. Cosmochim. Acta* **57,** 2699–2713.
Stipp S. L., Gutmannsbauer W., and Lehmann T. (1996) The dynamic nature of calcite surfaces in air. *Am. Mineral.* **81,** 1–8.
Sturchio N. C., Chiarello R. P., Cheng L., Lyman P. F., Bedzyk M. J., Qian Y., You H., Yee D., Geissbuhler P., Sorensen L. B., Liang Y., and Baer D. R. (1997) Lead adsorption at the calcite–water interface: Synchrotron X-ray standing wave and X-ray reflectivity studies. *Geochim. Cosmochim. Acta* **61,** 251–263.
Stumm W. and Morgan J. J. (1981) *Aquatic Chemistry,* 2nd ed. Wiley.
Teng H. H., Dove P. M., Orme C. A., and DeYoreo J. J. (1998) Thermodynamics of calcite growth: Baseline for understanding biomineral formation. *Science* **282,** 724–727.
Teng H. H., Dove P. M., and DeYoreo J. J. (1999) Reversed calcite morphologies induced by microscopic growth kinetics: Insight into biomineralization. *Geochim. Cosmochim. Acta* **63,** 2507–2512.
Tesoriero A. J. and Pankow J. F. (1996) Solid solution partitioning of $Sr^{2+}$, $Ba^{2+}$, and $Cd^{2+}$ to calcite. *Geochim. Cosmochim. Acta* **60,** 1053–1063.
Thorstenson D. C. and Plummer L. N. (1977) Equilibrium criteria for two components solids reacting with fixed composition in an aqueous phase—Example: The magnesian calcites. *Am. J. Sci.* **277,** 1203–1223.
Van Cappellen P., Charlet L., Stumm W., and Wersin P. (1993) A surface complexation model of the carbonate mineral-aqueous solution interface. *Geochim. Cosmochim. Acta* **57,** 3505–3518.
Van Cappellen P. and Qiu L. (1997a) Biogenic silica dissolution in sediments of the Southern Ocean. I. Solubility. *Deep-Sea Res. II* **44,** 1109–1128.
Van Cappellen P. and Qiu L. (1997b) Biogenic silica dissolution in sediments of the Southern Ocean. II. Kinetics. *Deep-Sea Res. II* **44,** 1129–1149.
van der Weijden R. (1995) Interactions between cadmium and calcite. Ph.D. thesis. Utrecht University.
Villermaux J. (1985) *Génie de la Réaction Chimique, Conception et Fonctionnement des Réacteurs.* Lauoiser Technique et Documentation.
White A. F. and Yee A. (1986) Near-surface alkali diffusion into glassy and crystalline silicates at 25°C and 100°C. In *Geochemical Processes at Mineral Surfaces* (eds. J. A. Davis and K. F Hayes), pp. 587–598. Symposium Series 323. American Chemical Society.
Zachara J. M., Kittrick J. A., and Harsh J. B. (1988) The mechanism of $Zn^{2+}$ adsorption on calcite. *Geochim. Cosmochim. Acta* **53,** 9–19.
Zachara J. M., Cowan C. E., and Resch C. T. (1991) Sorption of divalent metals on calcite. *Geochim. Cosmochim. Acta* **55,** 1549–1562.

## APPENDIX

### Aqueous Speciation

| Aqueous reaction[a] | Log K, 25°C, 1 atm, I = 0 |
|---|---|
| $2H^+ + CO_3^{2-} \Leftrightarrow H_2CO_3(aq)$ | −13.8 |
| $H^+ + CO_3^{2-} \Leftrightarrow HCO_3^-$ | 10.33 |
| $H_2O_{(l)} + CO_{2(g)} \Leftrightarrow 2\ H^+ + CO_3^{2-}$ | −18.16 |
| $Na^+ + H^+ + CO_3^{2-} \Leftrightarrow NaHCO3°$ | 10.08 |
| $Na^+ + CO_3^{2-} \Leftrightarrow NaCO_3^-$ | 1.26 |
| $Ca^{2+} + CO_3^{2-} + H^+ \Leftrightarrow CaHCO_3^+$ | 11.33 |
| $Ca^{2+} + H_2O \Leftrightarrow CaOH^+ + H^+$ | −12.60 |
| $Cd^{2+} + CI^- \Leftrightarrow CdCI^+$ | 1.98 |
| $Cd^{2+} + 2CI^- \Leftrightarrow CdCI_2$ | 2.60 |
| $Cd^{2+} + 3\ CI^- \Leftrightarrow CdCI_3^-$ | 2.40 |
| $Cd^{2+} + H_2O \Leftrightarrow CdOH^+ + H^+$ | −10.08 |
| $Cd^{2+} + 2H_2O \Leftrightarrow Cd(OH)_2° + 2H^+$ | −20.35 |
| $Cd^{2+} + CO_3^{2-} + H^+ \Leftrightarrow CdHCO_3^+$ | 11.83 |
| $Cd^{2+} + CO_3^{2-} \Leftrightarrow CdCO_3°$ | 3 |

[a] Sources: MINTEQA2 database (Allison et al., 1991), Fouillac and Criaud (1984), Stipp et al. (1993).